

## Spectroscopic Mode Mapping of Resonant Plasmon Nanoantennas

Petru Ghenuche,<sup>\*</sup> Sudhir Cherukulappurath, Tim H. Taminiau, Niek F. van Hulst, and Romain Quidant<sup>+</sup>  
*ICFO-Institut de Ciències Fotoniques, Mediterranean Technology Park, 08860 Castelldefels (Barcelona), Spain<sup>\*</sup>*  
*and ICREA-Institució Catalana de Recerca i Estudis Avançats, 08010 Barcelona, Spain*

(Received 15 February 2008; revised manuscript received 16 June 2008; published 9 September 2008)

We present spatially resolved spectral mode mapping of resonant plasmon gap antennas using two-photon luminescence microspectroscopy. The obtained maps are in good agreement with 3D calculations of the antenna modes. The evolution of the modal field with wavelength, both in the gap and along the two coupled gold nanowires forming the antenna, is directly visualized. At resonance, the luminescence for the gap area is enhanced at least 80 times and a comparison with the antenna extremities shows a dynamical charge redistribution due to the near-field coupling between the two arms.

DOI: [10.1103/PhysRevLett.101.116805](https://doi.org/10.1103/PhysRevLett.101.116805)

PACS numbers: 73.20.Mf, 73.21.-b, 78.67.Bf

Optical nanoantennas bridge the gap from the diffraction limit down to the nanometer scale, which offers unique advantages for novel photonic applications. Ideally, antenna concepts developed at radio frequencies can directly be scaled down to the optical regime because of the frequency invariance of Maxwell's equations. However, this downscaling raises technological challenges of nanoscale antenna fabrication and the optical properties of metals imply increased absorption losses. Fortunately the antenna performance can be substantially enhanced by plasmon resonances that lead to strong and confined fields [1,2] within the dielectric subwavelength gap between two resonant metal wire antennas. The overall enhanced optical response of such geometry was measured [3,4] and, recently, the increase of the quantum efficiency of dyes near gap antennas has been reported [5], opening the way to efficient nanolight sources and compact ultrasensitive sensing [6,7].

It is the local-field distribution at the antenna that determines its functionality, and different techniques have been used to study the spatial confinement and field enhancement around nanoantennas and in antenna gaps. Imura *et al.* applied scanning near-field optical microscopy (SNOM) on dispersed metal rods [8–10], and recently antennas have been imaged with scattering-type SNOM [11,12]. The high resolution snapshots of the local-field distribution are in fair agreement with theoretical predictions. However, the SNOM probe itself interferes with the intrinsic properties of the structure under study and affects the resonance conditions [13,14]. Therefore, approaches free of scanning tips are preferred, despite their intrinsic limited spatial resolution [15]. Recently we have exploited single molecules to probe the local field of a resonant antenna [16]. Nonlinear microscopy is particularly promising as the higher power dependence on the electric field makes the nonlinear response preferentially sensitive to the most intense fields close to the metal. In particular, two-photon induced luminescence (TPL) through interband transitions of gold provides a powerful method to study

gold antennas [17]. TPL microscopy has recently shown to be well suited to probe plasmonic fields around gold nanostructures [18,19] and gap antennas [3,4,20,21]. Despite the observed enhancement of the overall TPL signal from the antenna, the spectral extent of the resonant mode has remained unexplored. Moreover, the low spatial resolution so far has not allowed a direct correlation of the TPL signal with the spatial near-field distribution across the antenna.

In this Letter, we present mode mapping of individual and coupled gold nanowires, using TPL microscopy. By using a tightly focused laser beam we obtain spatially resolved TPL maps of the antenna response. These maps are found to be in very good quantitative agreement with calculated distributions of the modal local field to the fourth power. By scanning the excitation wavelength, the evolution of the TPL maps gives direct insight in the local-field enhancement due to the antenna resonance. By monitoring the spectroscopic evolution around the gap and along the antenna, we probe for the first time the dynamical modal field redistribution associated to the electromagnetic coupling of the two antenna arms.

Gold gap antennas have been fabricated by *e*-beam lithography onto indium tin oxide (ITO)-coated (10 nm) glass substrates. Each of the rods is 500 nm long, 100 nm wide, and 50 nm high while the gap between them has been fixed to 40 nm, with 10 nm accuracy. These dimensions enable us both to maximize the reproducibility of the fabrication process and to clearly resolve with our TPL setup the antenna gap from its edges. For comparison, we also fabricated 500 nm and 1  $\mu$ m long antennas (Fig. 1). The resonances of the antennas have first been determined by scattering spectroscopy (not shown). For an incident polarization along the long antenna axis (longitudinal polarization) the resonance of gap antennas is centered at 730 nm, slightly redshifted and broadened with respect to the resonance of isolated 500 nm rods at 710 nm, due to the near-field coupling [1]. While the 1  $\mu$ m long rods feature a main peak centered at 800 nm, their spectra appear more complex with a side shoulder at shorter wavelength. Under

transverse polarization all three geometries display a short-axis  $\lambda/2$  resonance peaking at around 600 nm.

In the TPL microscope, the antennas are illuminated by a tunable pulsed Ti:sapphire laser (150 fs pulses, 76 MHz repetition rate, 700–780 nm, average power  $30 \mu\text{W}$ ). To obtain the required spatial resolution, the beam is tightly focused by an immersion oil  $100\times$  objective with numerical aperture  $=1.25$  (illumination spot of  $\sim 350$  nm). The resulting intense local fields induce a two-photon absorption process in gold which leads to a wide-band photoluminescence emission [17]. The luminescence is collected back through the same objective and sent to an

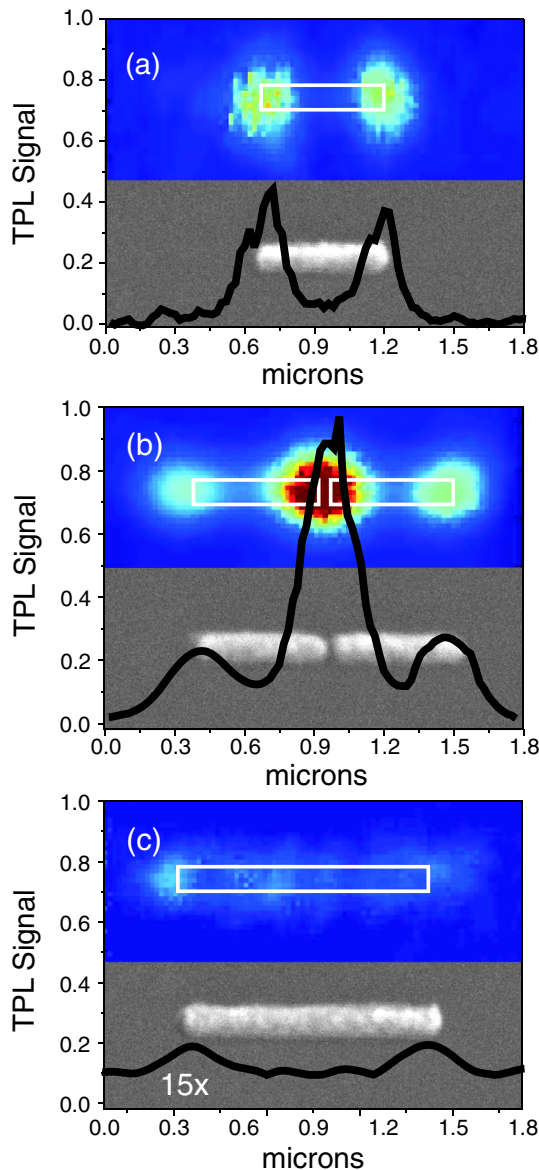


FIG. 1 (color online). TPL scans recorded on three different gold antennas and their respective scanning electron micrographs. (a) 500 nm bar, (b) coupled 500 nm antennas, and (c)  $1 \mu\text{m}$  bar. All measurements were performed at 730 nm under the same incident laser power.

avalanche photodiode after being filtered from the excitation light (detection window, 450–700 nm). Scanning the sample with respect to the illumination spot enables one to map the distribution of TPL intensity around the antenna. The optical resolution is about 200 nm, as determined by imaging isolated 100 nm sized gold particles. A systematic study of the influence of the size of the illumination focus and the collection area shows that the resolution and features of the TPL maps are mainly governed by the excitation path (not shown). Figure 1 shows TPL images recorded over the three antennas. Measurements are performed at 730 nm under longitudinal polarization, for which the gap antenna is resonant. For a single 500 nm gold bar, the TPL signal is concentrated at each of the extremities [Fig. 1(a)]. When coupled to form a gap antenna the TPL map becomes dominated by a substantial signal confinement and enhancement for the gap area [Fig. 1(b)]. For reference, it is instructive to look at the response of a continuous  $1 \mu\text{m}$  bar [Fig. 1(c)]. With almost 2 orders of magnitude weaker TPL signal, this measurement illustrates the absence of resonance at this wavelength and confirms that the resonant properties of gap antennas are governed by the resonance of each individual arm (detuned by coupling) rather than by an antenna of the same overall length.

To get insight in the relation between the measured TPL maps and the modal field distributions, we have carried out calculations based on the finite integral technique [22]. Figure 2(a) shows the distribution of the electric field for the resonant modes, excited by a plane wave, of the three antennas considered experimentally. To account for the actual shape of the fabricated structures, round corners with 30 nm radius are used, while calculating with a 2 nm mesh size. The glass substrate and the ITO layer have been included and the dielectric constant for gold taken from [23]. For all antennas, strong fields build up at the extremities of the bars. Moreover, for the gap antenna, the map is dominated by an even stronger field confine-

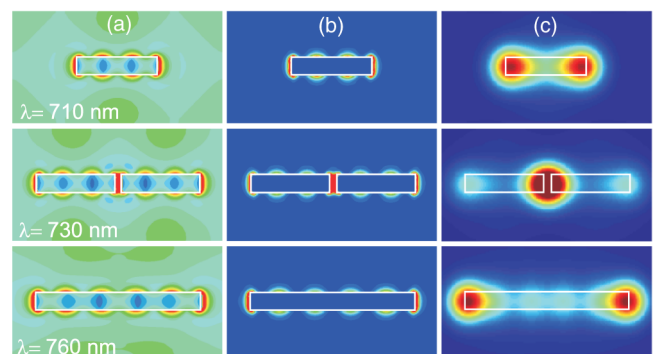


FIG. 2 (color online). Distribution of (a) the local field  $|E|$  and (b)  $|E|^4$  computed in the half-plane of the three types of antennas at their respective resonance wavelengths. (c) is obtained by convoluting the  $|E|^4$  maps with a 200 nm waist 2D Gaussian profile and integrating over the third dimension.

ment within the air gap. Additional weaker field modulations along the sides of the gold bars are signatures of the multipolar resonance involved. These modulations enable one to assign the modes associated to the resonances using the relation between the antenna length  $L$  and the effective wavelength  $\lambda_{\text{eff}}$ :  $L = (n + 1/2)\lambda_{\text{eff}}$  ( $n$  being an integer). The resonance of the isolated 500 nm bar at 710 nm is attributed to a  $3\lambda/2$  mode ( $n = 1$ ) with  $\lambda_{\text{eff}} = 333$  nm. The same  $3\lambda/2$  mode is shifted to 730 nm for a gap antenna. The  $1 \mu\text{m}$  bar features a  $5\lambda/2$  resonance ( $n = 2$ ) with  $\lambda_{\text{eff}} = 400$  nm when excited at 760 nm. Clearly, the gap-antenna mode is associated with the  $3\lambda/2$  mode of the isolated 500 nm bars. Owing to the quadratic dependence of the TPL signal with the local-field intensity, we are rather interested in  $|E|^4$  maps. To take the actual resolution of our setup into account, the maps are convoluted with a 2D Gaussian profile with 200 nm FWHM [Fig. 2(c)]. The resulting convoluted maps are fully dominated by the strong intensity in the gap and at the extremities.

Although the calculations of the local mode-field distributions are in general not equivalent to the experimental configuration, the excitation of the antenna mode at the discontinuities can be expected to be related to the strength of the local mode field. This reasoning is similar to the picture of mode excitation and scattering into radiation at the ends of long nanowires [24,25]. Upon comparison, excellent agreement is found between the TPL maps of Fig. 1 and the calculated modal distributions. This remarkable agreement indicates that TPL microscopy yields information on the spatial local-field distribution along the antenna. We proceed to analyze the spectral evolution of the TPL maps and quantitatively compare them to the calculated mode fields.

We have investigated the resonant behavior of the antenna modes by scanning the wavelength of the illuminating laser. For each wavelength, accounting for the transmittance of the optical setup, the laser power has been adjusted to maintain the power incident on the structure constant. Figure 3(a) shows the evolution of the TPL map recorded over a gap antenna when the wavelength is scanned from 710 to 770 nm in steps of 10 nm. For comparison, Fig. 3(b) shows the evolution of the corresponding convoluted  $|E|^4$  maps. The resonance at 730 nm is nicely reproduced, while the intensity decreases rapidly by moving only 30–40 nm out of resonance. The maxima at the extremities appear slightly shifted compared to the gap maximum, with a  $\sim 10$  nm blueshift in the experiment.

In Fig. 4 the spectra of the average TPL intensity in the gap area of the coupled antennas and at the extremities for the 500 nm and the  $1 \mu\text{m}$  bars are shown. In the same graph the corresponding maxima of the convoluted  $|E|^4$  maps are plotted. In very good agreement with the calculations, TPL spectroscopy enables one to retrieve the resonances of the local-field intensity around the different types

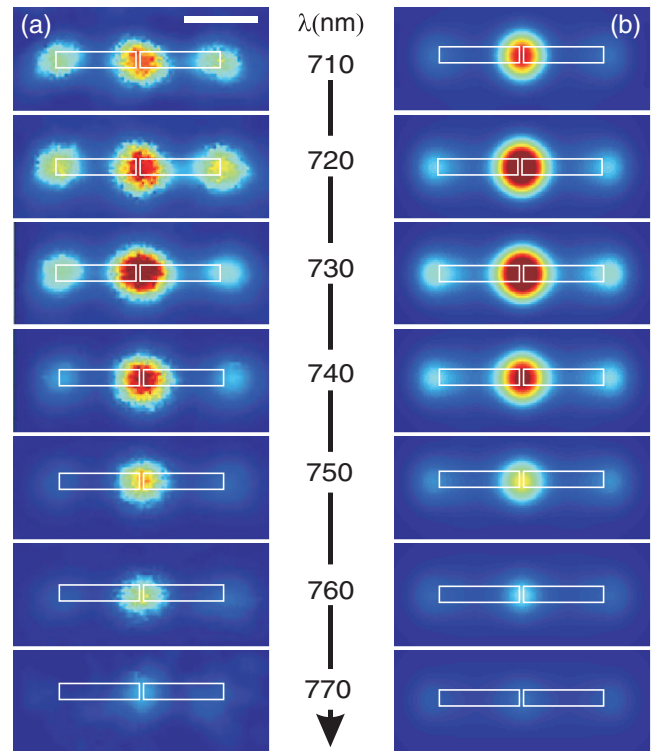


FIG. 3 (color online). Evolution with the incident wavelength of (a) the TPL map and (b) the computed convoluted  $|E|^4$  distribution over a single gap antenna (scale bar 500 nm).

of antennas and to determine their central wavelength and bandwidth. Interestingly, while the scattering measurements provide a resonance at around 800 nm for the  $1 \mu\text{m}$  antenna, the TPL spectrum shows the actual near-field resonance peaking around 760 nm, as also predicted by theory. This indicates that the complex far-field scattering pattern of the  $5\lambda/2$  mode leads to different spectral features compared to near-field spectroscopy [20,26,27].

Although the TPL intensity is clearly related to the local-field enhancement, it does not give a quantitative value. Considering the ratio between longitudinal and transversal resonances for a given antenna is not accurate since the comparison fully depends on the relative spectral position of both resonances [4]. Here TPL microspectroscopy provides an interesting alternative by calculating the ratio between the TPL in the gap area at resonance and away from it. Since the signal off resonance is given by the lowest value detectable from the noise level of our experiment, this leads to an estimation of a minimum value for the actual enhancement. This way, we find a TPL enhancement factor of at least 80 for the gap antenna versus 15 for the single antenna.

Beyond the evaluation of the local-field enhancement due to resonance, the combination of spatial resolution and spectral analysis of TPL spectroscopic imaging also enables a deeper analysis of the antenna physics. We plot in Fig. 4(d) the evolution with the incident wavelength of the

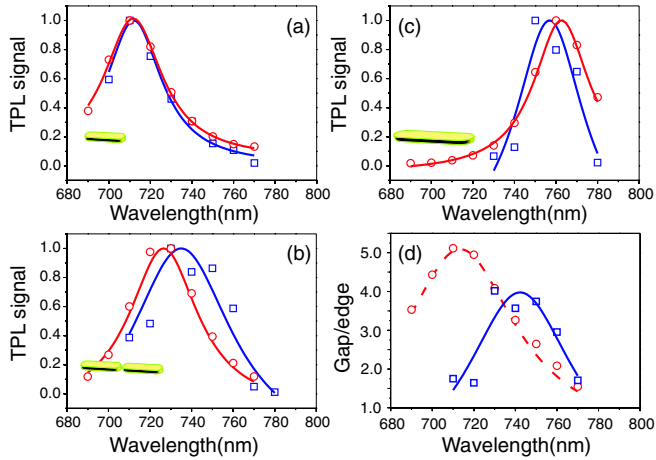


FIG. 4 (color online). Evolution with the incident wavelength of the TPL signal (blue squares) (a) for the extremities of a 500 nm bar, (b) the gap of a coupled antenna, and (c) the extremities of a 1  $\mu\text{m}$  bar. (d) The spectral evolution of the ratio between the signal in the antenna gap and at its extremities. The red circles account for the evolution of the corresponding calculated  $|E|^4$ . For comparison, all spectra have been normalized to unity (continuous lines are guides to the eyes).

ratio between the signal for the gap area and for the antenna extremities. This ratio features a peak centered around 740 nm for which the TPL response for the gap becomes up to 4 times stronger than at the edges. This effect is well reproduced by the corresponding  $|E|^4$  analysis, despite a small shift in wavelength mainly attributed to subtle shifts in the resonance maxima for the weak TPL intensity at the extremities. These results indicate that the coupling between the arms does not simply introduce a new mode, with a fixed charge distribution, whose amplitude is enhanced at resonance, as observed for a single bar. Instead, for the gap antenna, a dynamical redistribution of charge along the antenna is observed. We believe this constitutes the first experimental observation of the spectral evolution of the mode field of a coupled nanoantenna.

In conclusion, we have presented a systematic study by TPL microscopy of gold nanoantennas. TPL microscopy combines spatially resolving the main features of the antenna mode with a spectral analysis. Our results show how TPL scans can be directly compared with the convoluted distribution of the fourth power of the local electric field calculated with 3D simulations. By monitoring the evolution of the TPL distribution with the excitation wavelength we have assessed the near-field resonance features such as central wavelength and bandwidth. In good agreement with theoretical predictions, spectroscopic imaging has also

enabled us to deduce at least an order of magnitude enhancement of the local-field intensity in the gap area, at resonance compared to off resonance. Finally, we have uncovered in direct space the physical mechanism of field enhancement in the gap by showing a resonant behavior associated to a dynamic redistribution of charges.

This work was supported by the Spanish Ministry of Sciences through Grants No. TEC2007-60186/MIC and No. CSD2007-046-NanoLight.es and the CELLEX foundation.

\*Also at: The Institute for Space Sciences, Bucharest, Romania.

+romain.quidant@icfo.es

\*<http://www.icfo.es>

- [1] J. Aizpurua *et al.*, Phys. Rev. B **71**, 235420 (2005).
- [2] L. Novotny, Phys. Rev. Lett. **98**, 266802 (2007).
- [3] P. J. Schuck *et al.*, Phys. Rev. Lett. **94**, 017402 (2005).
- [4] P. Muhlschlegel *et al.*, Science **308**, 1607 (2005).
- [5] O. Muskens *et al.*, Nano Lett. **7**, 2871 (2007).
- [6] E. J. Smythe, E. Cubukcu, and F. Capasso, Opt. Express **15**, 7439 (2007).
- [7] S. Enoch, R. Quidant, and G. Badenes, Opt. Express **12**, 3422 (2004).
- [8] K. I. Imura, T. Nagahara, and H. Okamoto, J. Am. Chem. Soc. **126**, 12730 (2004).
- [9] K. I. Imura, T. Nagahara, and H. Okamoto, J. Phys. Chem. B **108**, 16344 (2004).
- [10] K. Imura and H. Okamoto, Opt. Lett. **31**, 1474 (2006).
- [11] E. Cubukcu *et al.*, Appl. Phys. Lett. **89**, 093120 (2006).
- [12] N. Yu *et al.*, Opt. Express **15**, 13272 (2007).
- [13] S. Mujumdar *et al.*, IEEE J. Sel. Top. Quantum Electron. **13**, 253 (2007).
- [14] A. F. Koenderink *et al.*, Phys. Rev. Lett. **95**, 153904 (2005).
- [15] N. Felidj *et al.*, Plasmonics **1**, 35 (2006).
- [16] T. H. Taminiau *et al.*, Nano Lett. **7**, 28 (2007).
- [17] M. R. Beversluis, A. Bouhelier, and L. Novotny, Phys. Rev. B **68**, 115433 (2003).
- [18] A. Bouhelier *et al.*, Phys. Rev. Lett. **95**, 267405 (2005).
- [19] A. Hohenau *et al.*, Phys. Rev. B **73**, 155404 (2006).
- [20] P. Ghenuche *et al.*, Appl. Phys. Lett. **90**, 041109 (2007).
- [21] D. ten Bloemendal *et al.*, Plasmonics **1**, 41 (2006).
- [22] CST Microwave Studio 5.1, [www.cst.com](http://www.cst.com).
- [23] *Handbook of Optical Constants of Solids*, edited by E. D. Palik (Academic, New York, 1985).
- [24] H. Ditlbacher *et al.*, Phys. Rev. Lett. **95**, 257403 (2005).
- [25] A. V. Akimov *et al.*, Nature (London) **450**, 402 (2007).
- [26] T. Søndergaard and S. I. Bozhevolnyi, Opt. Express **15**, 4198 (2007).
- [27] B. J. Messinger *et al.*, Phys. Rev. B **24**, 649 (1981).